

# Realization of a clock-based global height system: A simulation study for Europe and Brazil

Asha Vincent<sup>1\*</sup>, Jürgen Müller<sup>1</sup>, Christian Lisdat<sup>2</sup>, Dennis Philipp<sup>3</sup>

<sup>1\*</sup>Institute for Geodesy, Leibniz University Hannover, Schneiderberg 50,  
Hannover, 30165, Lower Saxony, Germany.

<sup>2</sup>Physikalisch-Technische Bundesanstalt, Bundesallee 100, Braunschweig,  
38116, Lower Saxony, Germany.

<sup>3</sup>ZARM, University of Bremen, Am Fallturm 2, Bremen, 28359, Bremen,  
Germany.

\*Corresponding author(s). E-mail(s): [vincent@ife.uni-hannover.de](mailto:vincent@ife.uni-hannover.de);  
Contributing authors: [mueller@ife.uni-hannover.de](mailto:mueller@ife.uni-hannover.de);  
[Christian.Lisdat@ptb.de](mailto:Christian.Lisdat@ptb.de); [dennis.philipp@zarm.uni-bremen.de](mailto:dennis.philipp@zarm.uni-bremen.de);

## Abstract

Chronometric levelling is a novel technique for the realisation of the International Height Reference System (IHRs). A detailed study of this technique is carried out through closed-loop simulations, aiming to unify regional/local height systems (LHS) in Europe and Brazil. Focusing on a unification accuracy of 1 cm, realistic scenarios with various error parameters/vertical datum parameters in LHS and clock observation uncertainties were analysed. The errors associated with local heights raised from datum offsets, local vertical datum alignment discrepancies in latitude and longitude, accumulated tilts depending on the distance from the reference tide gauge and levelling point elevation-dependent offsets were introduced. Clocks achieving a fractional uncertainty of  $10^{-18}$  and  $10^{-17}$  were assumed in the simulations, considering temporal correlations of clock intrinsic uncertainties, external effects on clock observations such as tidal effects, propagation delay in terms of link uncertainties and presence of outliers. We determine the preferred distributions of clocks in a network for the best estimation of error parameters. The estimation of the error parameters is related to the spatial distribution of the clocks, hence, an optimal setup of placing clocks at the most distant levelling points, reference tide gauges and elevated points is implemented. Further, a configuration of clock distribution is proposed with master clocks and local clocks with reduced links. Taking into consideration all these realistic constraints, a unification accuracy of 1 cm can be obtained. The unified European

and Brazilian height systems are further related to the global geoid such that all geoid-related heights achieve an accuracy of 3 cm.

**Keywords:** Chronometric levelling, Atomic clock, Global height system, Geopotential number, Unification of Height Systems, Vertical Datum Parameters

## 1 Introduction

The necessity of a global height system is paramount for various geodetic applications, such as infrastructure development across borders, disaster management, climate studies, etc. as it provides a globally consistent framework [1]. Regional height systems are established with respect to local vertical datums that are defined based on the local mean sea level at rest and determined at a reference tide gauge using the classical levelling technique and the GNSS/geoid approach [2]. Local datum points may not coincide with the global geoid due to several factors such as sea surface topography, ocean circulation, local currents and tides. Heights and derived quantities such as gravity anomalies, defined with respect to these local references, are inappropriate for international applications as they cannot be compared unless the transformation parameters or the vertical datum parameters between the local systems are known. Hence, the three pillars of Geodesy, Earth's geometry, rotation, and gravity field, defined in a physical reference system, offer consistency and reliability worldwide [3]. A reference system defined in relation to the Earth's gravity field supports the simultaneous determination and monitoring of the geodetic parameters [4].

Current unification techniques for the IHRS involve integrating spaceborne and terrestrial gravity data, along with precise geodetic positioning using GNSS and advanced satellite gravimetry (e.g., GRACE and GOCE). The target accuracy for vertical station positions is  $\pm 3$  cm (1 cm long-term), and  $\pm 0.03 \text{ m}^2/\text{s}^2$  for geopotential differences at the global level. The use of highly precise atomic clocks, especially optical clocks, offers a promising approach for directly measuring gravity potential differences between the locations of interest. This method provides a direct link to geopotential numbers, overcoming the limitations of traditional height determination techniques [5, 6]. By comparing clock frequencies at different sites, gravity potential and height differences can be determined with enhanced accuracy, detecting small variations in near real-time, something satellite missions cannot achieve [7, 8]. An International Height Reference System (IHRS) can be established with a proper network of atomic clocks, either by unifying existing local systems with the aid of clock observations or by fixing a frame which is (entirely) based on distributed atomic clock networks – a chronometric reference frame. Those networks can also be used for, e.g., monitoring mass redistribution and surface deformations [6, 9].

## 2 IHRS Realization through Chronometric Levelling

Refs. [10] and [9] state five conventions that define the IHRS, which was issued in the IUGG (International Union of Geodesy and Geophysics) 2015 General Assembly. The

vertical coordinate of a point  $P$  is the geopotential number  $C_P = W_0 - W_P$ , which is the difference between the gravity potential at the geoid  $W_0$  and at the point of interest  $W_P$ <sup>1</sup>. Hence,  $C_P$  provides the effective or actual potential difference at the point  $P$  that includes geoid height variation and surface deformation at the measurement epoch [7, 11]. A clock comparison determines the difference in elapsed proper times or the relative frequency difference, the redshift, between two clocks. The redshift of two standard clocks<sup>2</sup> is affected by the individual positions in the gravity field and the relative state of motion. In the case of two Earth-bound (stationary) clocks, the second part is related to the centrifugal potential. In the following, we always assume that all involved clocks are indeed standard clocks. All experiments to date agree that atomic clocks are standard clocks. In a post-Newtonian approximation, i.e., at the accuracy of  $1/c^2$  with  $c$  being the speed of light, the redshift  $z$  or the relative fractional frequency difference between clocks at sites 1 and 2 corresponds to the difference in height  $\Delta H$  between the two sites,

$$z = \frac{\Delta f}{f} \approx \frac{\Delta W}{c^2} \approx \frac{g\Delta H}{c^2}, \quad (1)$$

where  $f$  represents the frequency,  $\Delta W = W_1 - W_2 = C_2 - C_1$  is the corresponding gravity potential difference [12–16] and  $g$  is the gravity acceleration. In equation (1),  $W$  is the Newtonian gravity potential. Note that a generalized equation is available that holds at all orders in full general relativity, see e.g., [17, 18]. For two stationary clocks being virtually on the geoid and at a surface point  $P$ , respectively, the fractional frequency difference would provide a direct measurement of the geopotential number  $C_P$ ,

$$z = \frac{\Delta f}{f} \approx \frac{C_P}{c^2} \approx \frac{gH_P}{c^2}, \quad (2)$$

where  $H_P$  is the height of point  $P$  above the geoid. High-performance clocks of fractional uncertainty  $10^{-18}$  as already realized in labs at, e.g., PTB (Physikalisch-Technische Bundesanstalt), NIST (National Institute of Standards and Technology), JILA (Joint Institute for Laboratory Astrophysics), or at the National University of Singapore [19–21], are sensitive to a potential variation of  $0.1 \text{ m}^2/\text{s}^2$  or a corresponding height difference of 1 cm close to the Earth’s surface [22, 23].

### 3 Basic Methodology

We have adopted the approach described in [5] and run dedicated simulations for quantification. For the following, the framework of the first-order post-Newtonian theory for clock comparison is employed. The a priori height system, which is considered to be the unified system, is subdivided into several LHS with respect to their reference tide

---

<sup>1</sup>Note that the positive sign convention is used, in which the geopotential  $W$  is always positive and limits to zero at infinite distance from the mass concentration.

<sup>2</sup>In relativity, a standard clock is a clock that measures its own elapsed proper time, which is the four-dimensional length of its worldline in spacetime.

gauges. The basic idea is the unification of local heights using a clock-based adjustment procedure, assuming realistic conditions. Closed-loop simulations are carried out using local heights and clock measurements as observations to estimate the unified heights along with the transformation parameters between the LHS. We propose a certain number of clocks  $n$  distributed in each LHS with several connections between them. The number of clocks must be greater than the total number of to be determined error parameters to ensure (over)determined solutions. If all clocks are interconnected, we can have a total of  $\binom{n}{2}$  observations. This larger number can allow for a reduction of measurement errors related to the clock and link uncertainties, depending on the correlations between the different effects in the respective measurements in the observations. The accuracy of the unification is determined by comparison to the a priori height values. The research focus for the Europe-only and the Brazil-only cases has been different. In Europe, the study concentrates on realistic and complex error parameters between LHS, optimal number and spatial distribution of clocks, and unification with different frequency standards. The number of clock links and their uncertainties, outlier effect, and correlations are the focus in Brazil.

### 3.1 Data Preparation

In order to simulate clock observations as the gravity potential differences, we require either the direct value of  $C_p$  of the levelling points in the height systems or the normal heights  $H^N = \frac{C_p}{\bar{\gamma}}$ , where  $\bar{\gamma}$  is the mean normal gravity value along the normal plumb line associated with the level ellipsoid [11]. The European Vertical Reference Network (EUVN) height solution for which the vertical datum is related to NAP, provides normal heights all over Europe [24]. With the computed value of  $\bar{\gamma}$ ,  $H^N$  of each levelling point is transformed to the corresponding potential number  $C_p$ . Brazilian levelling data in terms of  $C_p$  were obtained from the working group of SIRGAS, the Geocentric Reference System for the Americas.

### 3.2 Local Heights With Complex Error Parameters

Considering realistic cases, different scenarios of local height observation equations were built considering complex vertical datum parameters. The errors associated with local heights raised from datum offsets ( $OT^L$ ), local vertical datum alignment discrepancy in the latitude and longitude directions ( $a^L$  and  $b^L$ ), accumulated tilt depending on the distance from the reference tide gauge ( $t^L$ ), levelling point elevation-dependent offset ( $m^L$ ) were introduced. By assuming a random noise ( $RN$ ) along with the offsets and systematic tilts that exist between the LHS with respect to the pre-defined reference datum, local height values (in terms of gravity potential differences,  $C_P$ ) are generated. The local height ( $H_i^L$ ) observations in terms of geopotential numbers ( $C_i^L = gH_i^L$ ) generated by including all of these errors can be represented as

$$C_i^L = C_i^U + (a^L \Delta X_i + b^L \Delta Y_i + t^L \Delta S_i) \cdot g + m^L C_i^U / E + OT^L + RN, \quad (3)$$

where  $\Delta X_i$  is the latitude distance in degree,  $\Delta Y_i$ , is the longitude distance in degree,  $\Delta S_i$ , is the distance from the tide gauge in degree and,  $E$  ( $= 500$  m) is the constant

height value that determines the elevation dependent offset. An elevation step of  $E = 500$  m is chosen as an arbitrary value that determines the offset ranges. If there are no points with elevations greater than 500 m, we assume that the contribution to the error from this offset is negligible and can be ignored. Random noise in the range of  $0.1 \text{ m}^2/\text{s}^2$ , which is equivalent to 1 cm, is used for clocks with fractional uncertainties of  $10^{-18}$  and similarly  $1 \text{ m}^2/\text{s}^2$  for uncertainties of  $10^{-17}$ .

### 3.3 Realistic Clock Observations

A clock observation is affected by clock intrinsic errors ( $CE$ ) from the two clocks that can be time-correlated, clock comparison uncertainties ( $PD$ ) and external effects such as tidal effects ( $TE$ ). The observation equations for clock measurements ( $\Delta W_{ij}$ ) are generated from the a priori  $C_i^U$ ,

$$\Delta W_{ij} = -(C_i^U - C_j^U) - (TE_i - TE_j) + PD_{ij} + CE_i + CE_j, \quad (4)$$

where  $i$  and  $j$  represent the clock sites. We assume high-performance clocks with clock errors  $CE$  between  $10^{-17}$  and  $10^{-18}$  as outlined in the respective sections.

#### 3.3.1 Clock Intrinsic Uncertainties and Time Correlation

Clocks have a random frequency offset, within their uncertainty, from the true, unperturbed frequency. Depending on their origin, these offsets can vary between campaigns or be constant in time. The latter introduces correlations between the clock observations, while the former leads to a reduction of the influence of clock errors on the unification accuracy by averaging, if the observations are not simultaneous. Generally, we assume that the frequency offset of each clock is constant within each observation, but uncorrelated between different observations using this clock. In Sec. 4.2.4, we discuss a scenario for Brazil with correlated clock errors when the same clocks are involved within the same LHS.

The clock-related statistical noise can be reduced by a sufficiently long averaging time ( $\tau$ ) below the systematic uncertainties  $CE_i$  of the clocks. Depending on the type of optical clocks and their uncertainties, averaging times between several hours and several days are required to achieve this. These are still reasonable numbers, which is why we assume that this noise contribution can also be neglected against the clock uncertainty by taking daily averages ( $\tau \approx 10^5$  s).

#### 3.3.2 Clock Comparison Uncertainties

For the uncertainties that originate from the clock comparison ( $PD$ ), we consider two independent contributions: noise originating from the signal distribution, i.e. the link, and systematic errors from the link. Which contributions to  $PD$  are significant depends on the type of link used for the clock observation and its averaging time. If optical interferometric fibre links [25] are used to compare clocks, the situation can be strongly simplified. Typically, link noise reduces much faster with averaging time than the clock-related noise [26], and the latter dominates when averaging longer than 100 s. Furthermore, the link's systematic error values in the order of  $10^{-19}$  can be

reached under realistic field conditions, as it was demonstrated in loop configurations [27]. In consequence, we can neglect the link contributions compared to the systematic clock uncertainties  $CE_i$ .

When no interferometric fibre links are available because of missing infrastructure or too long distances, clock connections need to be realized by free-space links, typically to space. Such links exist and employ different microwave technologies to link clocks [28] and can reach low- $10^{-17}$  uncertainties [29, 30]. Optical links are under development [31, 32], but not yet in use on or to satellites. These links typically exhibit higher instability than interferometric fibre links and require longer averaging times to reduce statistical noise contributions. A promising tool for global clock comparisons will soon become available by the ACES mission [33], which will allow for global frequency transfer with uncertainties as low as  $\approx 5 \times 10^{-17}$ . According to [34], the uncertainty contribution of the ionospheric delay to the space link is in the order of  $5 \times 10^{-19}$ . We consider different cases for uncertainties of free-space links: presently realistic numbers of  $10^{-17}$  as well as more optimistic ones for future optical links with  $10^{-18}$  uncertainty. These uncertainties are dominating in  $PD$ . The applied values are given in the discussion of the respective scenario below (Sec. 4.2.2).

### 3.3.3 Tidal Effects on Clock Observations and their Correction

In a real-world scenario, clock observations are affected by the fluctuating Earth's gravity potential including external factors like tide-generating potentials and accurate reductions are required. The major tidal effects are solid-earth tide (SET) and ocean

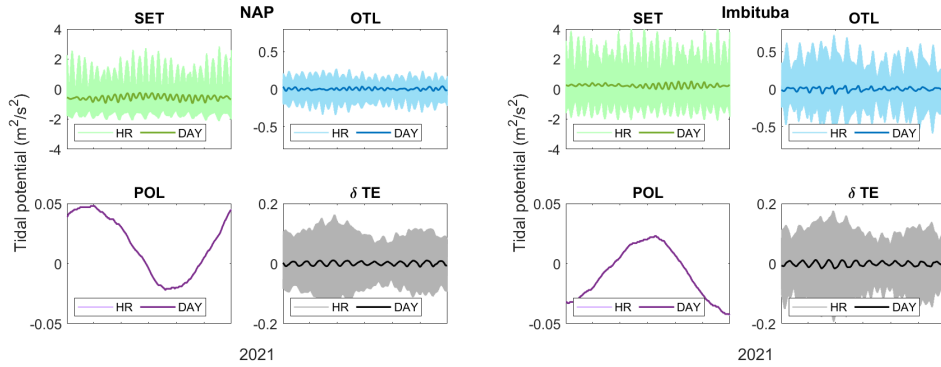


**Fig. 1:** Hourly and daily potential variations due to solid earth tide (SET), ocean load tide (OTL) and pole tide (POL) with corresponding model error ( $\delta TE$ ) at NAP (Normaal Amsterdam Peil), datum point of European system (left) and Imbituba, the datum point of Brazilian system (right).

tidal loading (OTL) caused by the Sun, Moon, and other celestial objects [35]. Centrifugal effects of polar motion generate the pole tide (POL) and, length-of-day tides (LOD) by the variations of Earth's angular velocity [36]. Also, atmospheric tides [37]

have to be considered. The LOD and atmospheric tidal potentials can be neglected as their range is below clock sensitivity  $10^{-18}$  ( $\approx 0.1 \text{ m}^2/\text{s}^2$ ) [38]. A modified version of the ETERNA34 (PREDICT program) Earth tide data processing package [39] with the HW95 (Hartmann and Wenzel 1995) tidal potential catalogue (TGP) is used to model hourly SET and POL tidal potential variations. The corresponding hourly OTL values with respect to EOT11a (Empirical Ocean Tidal Model) [40] were generated using the SPOTL3.3.0.2 package [41].

We model tidal effects  $\Delta C_i(t)$  in terms of variations in  $C$ . An assumption was made that all clock observations were carried out in the year 2021, for which the daily tidal effects are computed by averaging the modelled hourly solutions as clock observations are also assumed to be daily averaged. To simulate the model errors, tidal potential variations were estimated using different models of the TGP catalogue (Tamura87) and ocean tide model (FES2004). The estimated model differences ( $\delta TE_i$ ) are added as additional errors with the tidal potential values  $\Delta C_i(t)$

$$TE_i = \Delta C_i(t) + \delta TE_i, \quad (5)$$

The tidal potential values vary depending on the latitude. Hourly tidal potential variations (SET+OTL+POL) between the clock sites in the order of  $[-4 \text{ to } 4] \text{ m}^2/\text{s}^2$  average down to  $[-0.4 \text{ to } 0.4] \text{ m}^2/\text{s}^2$  over a day. Similarly, the model error  $\delta TE$  reduces from  $\approx 0.1 \text{ m}^2/\text{s}^2$  to  $\approx 0.02 \text{ m}^2/\text{s}^2$  when daily averages are taken from hourly solutions. Tidal potential variations generated at the datum points of the European system (NAP) and Brazilian system (Imbituba) are shown in Fig. 1. Short-baseline clock comparisons are less affected by tidal effects since they experience similar influences, reducing their differential impact. During the height system unification, we correct the clock observations  $\Delta W_{ij}$  for the respective estimates of the tidal influences  $\Delta C_{i,j}$ . In consequence, the clock observations are only influenced by the model errors  $\delta TE$ .

## 4 Results and Discussions

### 4.1 European Height System – Relation to NAP

For the simulation, 202 levelling points from the EUVN2000 perturbations defined by the model in Eq. (4) were added to generate a realistic topology. We classified these points into four local systems, G1, G2, G3 and G4 (Fig. 2). The rationale behind the added perturbations is based on [42] and [5]. As we have assumed a total of 5 different errors in each LHS, the total number of unknown parameters equals 18. The offset  $OT^{L3} = 0$  as the pre-defined unifying datum is NAP, the local vertical datum of G3.  $m^{L2} = 0$  because there are no high elevated points ( $> 500 \text{ m}$ ) in G2. With five clocks of  $10^{-18}$  uncertainty in each LHS and all clocks being interconnected, we have a total of 190 clock observations. The clock uncertainties between these observations are treated as uncorrelated. Unification is carried out using a least-squares adjustment with the observation equations mentioned in sections 3.2 and 3.3. The specific distribution of the clock network is discussed in detail in Sec. 4.1.1. The unification results obtained are shown in Fig. 3. The difference between unified heights and a prior heights is

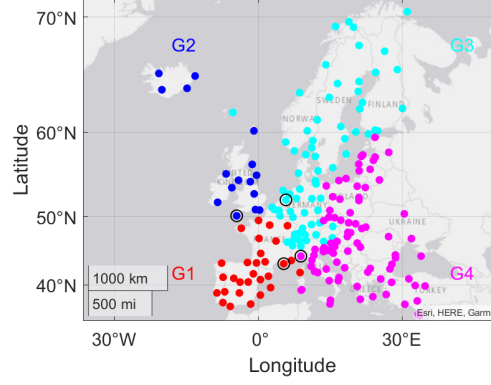


**Fig. 2:** Classified EUVN height system. The 4 LHSs, G1, G2, G3, and G4 are indicated in different colours. The reference tide gauges for each LHS are marked by black circles.

provided as residual error in Fig. 3 (right). The overall unification accuracy for each LHS is in the order of 1 cm (Tab. 1).

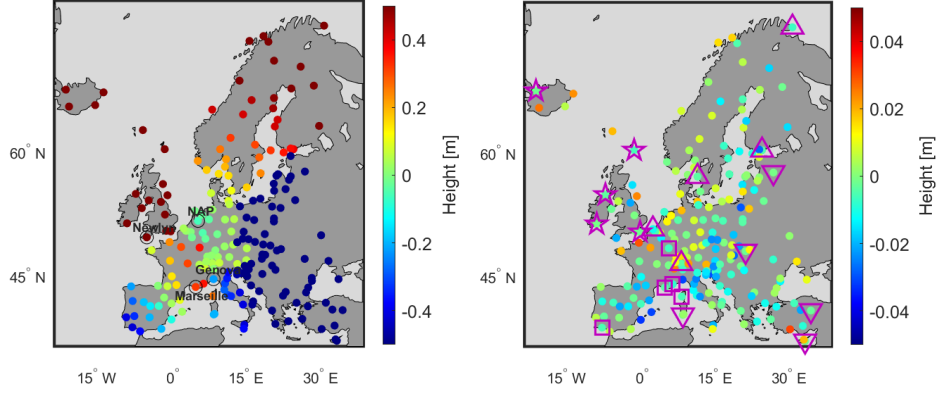


**Fig. 3:** True error before unification (left) and the residual errors after unification (right) obtained with the extended model. Different symbols represent the clock sites in each LHS. The errors reduced to  $\approx \pm 1$  cm after the clock-based unification.

**Table 1:** RMS error of each LHS after unification

LHS	G1	G2	G3	G4
RMS Error (cm)	1.46	1.37	1.09	1.33



#### 4.1.1 Clock Network Configuration

For the estimation of error parameters within each LHS, the spatial distribution of clocks plays a crucial role. Specifically, to accurately estimate tilt values, clocks should be strategically placed at both the maximum and minimum points of the tilt within the local height system. Conversely, for precise offset estimation, clocks should be

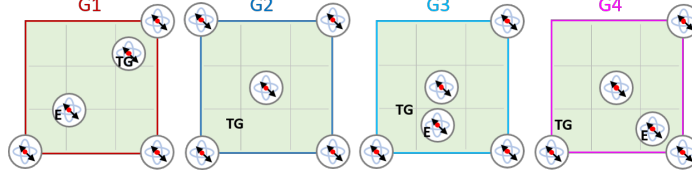


**Fig. 4:** Spatial distribution of 5 clocks associated with as used in each LHS – G1, G2, G3 and G4. The preferred clock positions are at the four corners, tide gauge (TG), maximum elevated point (E) and LHS centre.

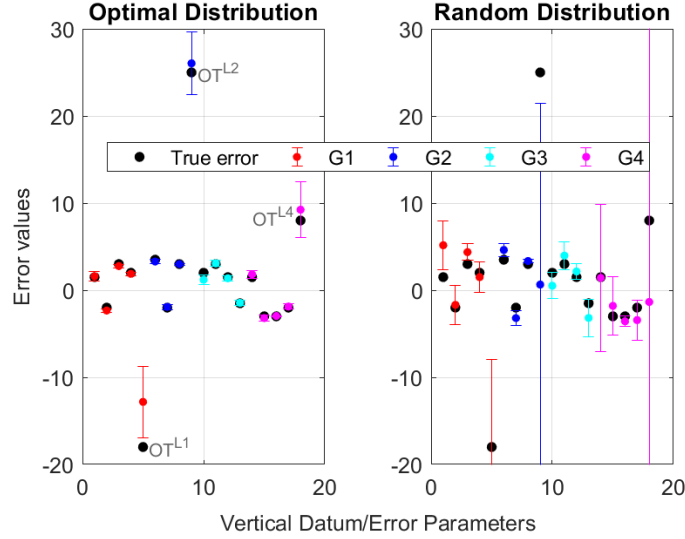


**Fig. 5:** Estimated error parameters in an extended model with a total of 18 unknowns with their standard deviations for an optimized distribution (left) and clocks operated at five levelling points that were randomly chosen from pool in each LHS (right). The assumed true error values are provided for reference. The units are different for tilts (cm/degree) and offsets (cm).

positioned at points least affected by tilts. As the tilts are direction-dependent, the most northerly, southerly, easterly and westerly points of each LHS, where  $a^L \Delta X$  and

$b^L \Delta Y$  mostly have extreme values that can serve as clock sites for better estimation of  $a^L$  and  $b^L$ . A clock near or at the reference tide gauge site can help in estimating  $t^L$  more accurately. A clock at the highest elevated point in the LHS, where  $m^L C^U/E$  is maximum, allows an accurate estimation of  $m^L$ . Thus, the optimal spatial arrangement of clocks is contingent upon the nature of systematic tilts and offsets present within the system. The idea is that tilts are direction-dependent, and clocks can be placed at the most extreme points to capture them. One can also get some a priori knowledge of these distortions through GNSS/levelling and geoid comparisons [43].

Therefore, we assumed a spatial distribution with five clocks as demonstrated in figure 4. This optimized configuration has the minimal standard deviations of the estimated error parameters ( $a^L, b^L, c^L, t^L, m^L, OT^L$ ) while analyzing the covariance matrices after several unifications with different network configurations (Fig. 5 (left)). Hence, the optimal configuration is suggested to determine the assumed (realistic) error parameters if real clock campaigns are run. The corresponding values associated with a random distribution are also provided (Fig. 5 (right)) for comparison. This spatial arrangement ensures that the unification process achieves high accuracy with minimal uncertainty. The largest deviation in the error determination ( $OT^{L1}$ ) obtained with the optimal configuration is  $\approx 5$  cm for  $OT^L/g$  and  $\approx 1$  cm for  $m^L$ . For tilts ( $a^L, b^L, t^L$ ) the values below  $\approx 1$  cm/degree. We are not limited to fixed/lab clocks in this procedure, as campaigns with  $10^{-18}$  transportable clocks are sufficient for the unification process.

#### 4.1.2 Clocks with Different Frequency Uncertainties

As an alternative to the scenario with only high-performance clocks with errors of  $10^{-18}$ , we consider a situation with mixed clock uncertainties in the local systems. Each LHS contains two  $10^{-17}$  clocks and two  $10^{-18}$  clocks; the height observation equation (3) is applied considering a simplified model including 3 biases –  $a^L$ ,  $b^L$ , and  $OT^L$  (other tilts are set to zero) – in each LHS. The unification accuracy is better when the more accurate clocks ( $10^{-18}$ ) are placed at the lower and upper extreme points diagonally. The comparison of the overall accuracy associated with the diagonal (I) and off-diagonal (II) distribution of more accurate clocks is provided in Tab. 2. This difference can be associated with the nature of the assumed error parameters. Hence, the lower extreme and upper extreme points possess the minimal and maximal tilts in the simplified model. The clock at the lower extreme point is only affected by an offset, possibly indicating better efficiency in estimating the error parameters. The true error before unification and the adjusted error after unification are shown in Fig. 6. Note that a unification accuracy of  $\approx 1$  cm can still be achieved with a network combination of  $10^{-18}$  and  $10^{-17}$  clocks in each LHS if a sufficient number of uncorrelated clock observations are available.

**Table 2:** RMS error of each LHS after unification

LHS	G1	G2	G3	G4
RMS Error I (cm)	1.38	2.10	1.09	1.95
RMS Error II (cm)	2.13	3.05	4.07	3.13

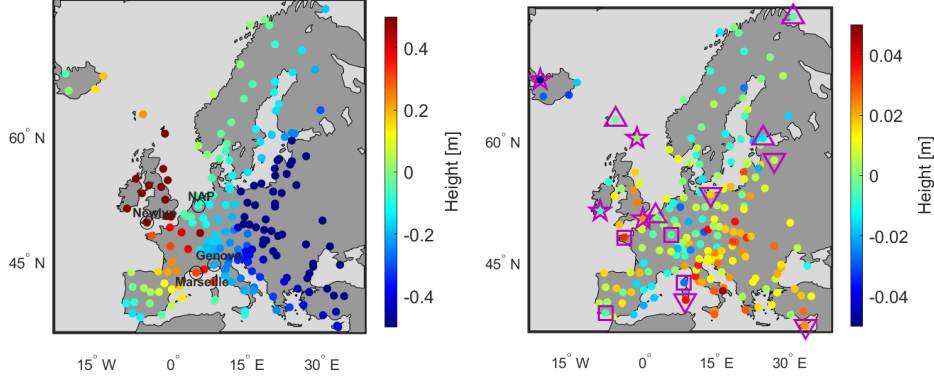


**Fig. 6:** True error before unification (left) and residual errors after unification (right) when clocks with different frequency uncertainties are used in each LHS with more accurate clocks ( $10^{-18}$ ) placed at lower extreme points and upper extreme points diagonally. Different symbols in the right image represent the clock sites in each LHS. The errors reduced to  $\approx \pm 1$  cm after clock-based unification.

## 4.2 Brazilian height system – Unify to Imbituba

We have access to a total of 71196 geopotential numbers of Brazilian levelling data. To

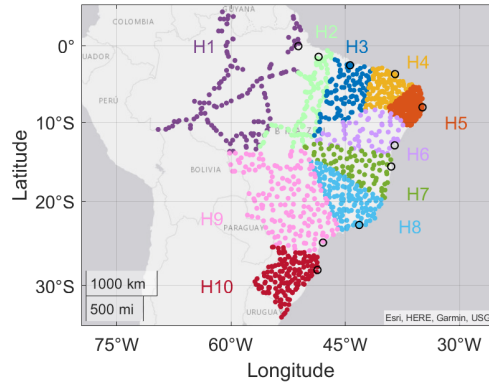


**Fig. 7:** Classified Brazilian height system. The 10 LHSs: H1, H2, H3, H4, H5, H6, H7, H8, H9, and H10 are indicated in different colours. The reference tide gauge locations for each LHS are indicated by a black circle.

simplify the simulation by reducing the number of levelling points, different grid sizes are defined for each LHS for the selection of fewer points and reduced to a total of 1164 geopotential numbers, because this smaller number of levelling points is still sufficient to accurately represent the topology in Brazil. Based on the tide gauge coordinates

obtained from PSMSL (Permanent Service for Mean Sea Level), all points are classified into 10 LHS by assigning a reference tide gauge to each of the LHS, see Fig. 7. Thus, we have a set of 10 LHS: H1, H2, H3, H4, H5, H6, H7, H8, H9, and H10 which have to be unified with the datum of H10, Imbituba as reference. Here, the height observation

**Table 3:** True errors in the 10 LHSs of the Brazilian system before unification

Error parameters	H1	H2	H3	H4	H5	H6	H7	H8	H9	H10
$a^L$ (cm/degree)	2	1.5	-2	1.5	3	2.5	2	2	3.5	3
$b^L$ (cm/degree)	3	2	2	-1.5	2.5	-3	1.5	2.5	2	3
$OT^L/g$ (cm)	-34	6	22	-28	30	26	15	-10	35	0

equation is applied by a simplified model including only 3 errors ( $a^L$ ,  $b^L$ , and  $OT^L$ ) in each LHS, resulting in a total of 29 unknown transformation parameters ( $OT^{L10} = 0$ ). The assumed error budget in each LHS is provided in Table 3. A network of 4 clocks with uncertainties of  $10^{-18}$  distributed at the four extreme points of the LHS with a reduced number of connections is considered. This provides a sufficient number of clock observations to determine the unknown parameters with high accuracy.

#### 4.2.1 Modified Clock Links

Rather than discussed in [5] and Sec. 4.1, where all clocks are inter-connected, the

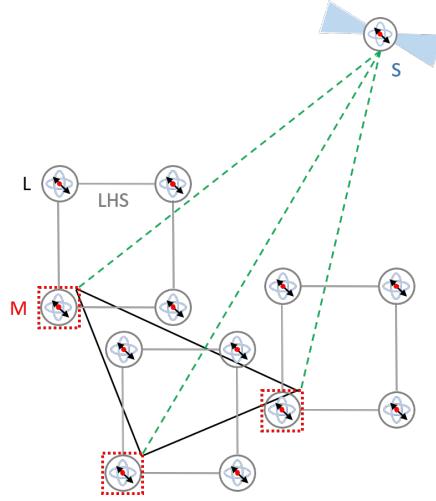


**Fig. 8:** Configuration of clock distribution with master clocks (M) and local clocks (L) in each LHS. Local clock connections were established with fibre links within the LHS. Master clocks of each LHS can be connected via either optical fibre (black) or free-space links (green).

number of links and thus clock observations can be reduced without considerably affecting the accuracy of the unification. This is explained by the number of clock observations in each LHS, that is similar to the case in Europe, which leads to a comparable reduction of uncorrelated clock errors by averaging the observations. We propose a configuration of clock networks with one master clock in each LHS that is connected to all other master clocks (M), and the local clocks (L) are connected to each other internally within their respective LHS (Fig. 8). Thus, with 4 clocks in each LHS, we have 60 local links ( $10 \cdot \binom{4}{2}$ ) and 45 master links ( $\binom{10}{2}$ ) in such a reduced link configuration. Optical fiber links ( $10^{-19}$ ) uncertainty for local clocks and free-space links ( $10^{-18}$ ) for master connections are assumed. The connections are reduced such that there exist single connections from each LHS to any other LHS through the master clocks only, which assumes a space link in our study.

#### 4.2.2 Propagation Delay in Terms of Link Uncertainty

In Sec. 3.3, details on the formulation of expected link uncertainty during clock comparisons can be found. In our simulations, local clock connections are always assumed as optical fibre links, with uncertainty in the order of  $10^{-19}$ , i.e., local links are dominated by the clock uncertainty. Unification results with different uncertainties on the master links ( $10^{-17}$  and  $10^{-18}$ ) are shown in Fig. 9. A unification accuracy of 1 cm can be achieved when  $10^{-18}$  space links and  $10^{-19}$  fibre links are employed in the specified link configuration. The overall accuracy in each LHS is provided in Tab. 4 for the two cases.

**Table 4:** RMS error of each LHS after unification

LHS	H1	H2	H3	H4	H5	H6	H7	H8	H9	H10
RMS Error (cm) $10^{-18}$ space link	1.08	1.23	1.03	1.43	1.37	1.42	1.13	1.29	1.19	2.43
RMS Error (cm) $10^{-17}$ space link	18.0	17.1	13.0	12.3	9.83	7.82	6.56	4.88	2.95	1.39

#### 4.2.3 Robust Parameter Estimation Approach

The possibility of outliers in real clock observations cannot be neglected. Reducing clock links to a total of 105 observations and subsequently removing or down-weighting outlier observations can significantly impact the accuracy of unification, as the number of reliable observations diminishes. To analyze this effect, an outlier model is introduced by adding a certain number of outliers to the clock observations (in the order of  $50 \text{ m}^2/\text{s}^2$ ). The impact of different outlier distributions on the results can be assessed by varying the number and placement of the outliers. Outliers can be removed (weight = 0) or down-weighted (Huber’s iteratively reweighting algorithm [44]) during unification with the aid of an outlier detection method. The adjusted error after unification with two scenarios, when the outlier model is applied to all links and only to master

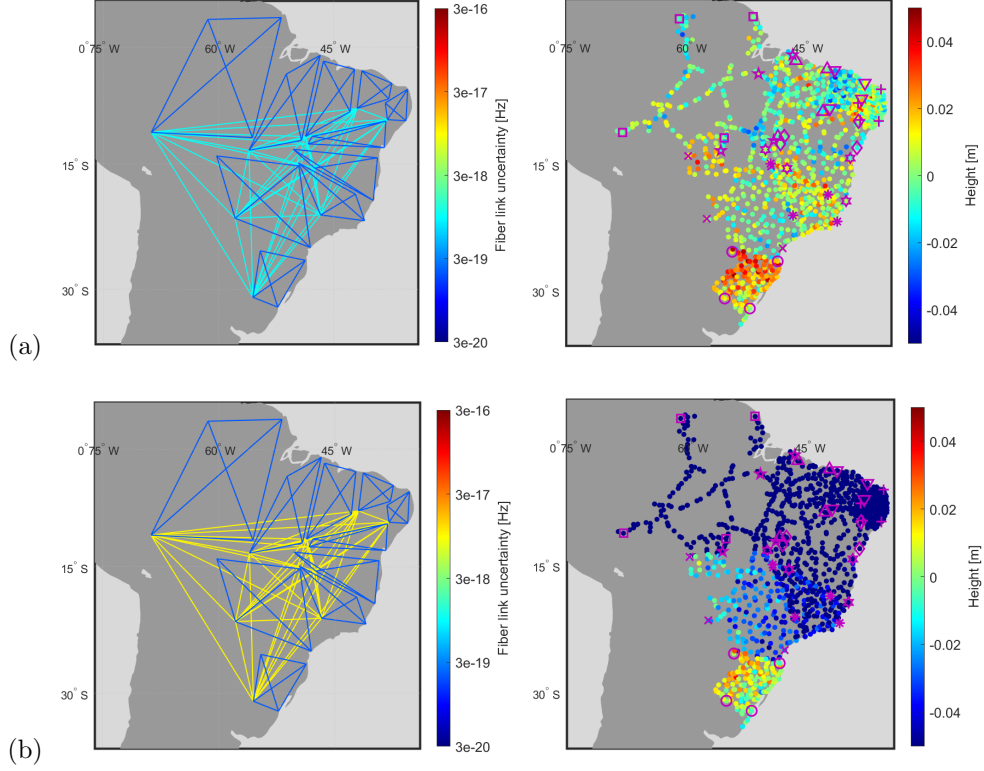


**Fig. 9:** Link uncertainty (left) and adjusted error (after unification) (right) with different cases of free-space master clock connections. In all cases, local connections are assumed as precise optical fibre links ( $10^{-19}$ ). All master links are assumed as  $10^{-18}$  free-space links (a) and  $10^{-17}$  free-space links (b). Residuals are smaller, in the range of 1 cm, when  $10^{-18}$  space links are assumed.

links, is shown in Fig. 10. Reducing the reliable local links affects the unification accuracy. A unification accuracy of 1 cm can still be achieved if we can assume outlier-free local links, which can be achieved with fibre links.

#### 4.2.4 Time Correlations in Clock Observations

In clock-based height unification, the impact of time correlations in clock observations was analysed. With four clocks per local height system (LHS), each pair of clocks is linked, generating six clock observations per LHS. However, due to correlations between these local links with the same clock, the effective number of independent observations is reduced to three (Figure 11) This reduction highlights the need to account for correlation structures in the adjustment process, as time correlations affect the covariance matrix and the estimation of the transformation parameters such as offsets ( $OT^L$ ) and tilts ( $a^L, b^L$ ).

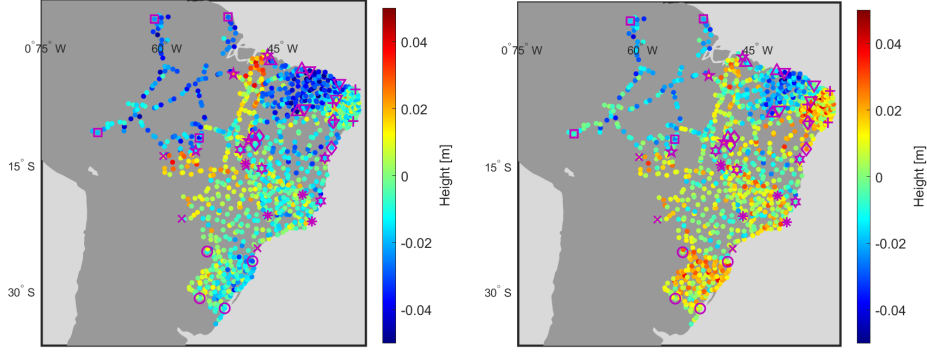


**Fig. 10:** Adjusted error after unification when Huber's RPE method is applied with outliers distributed among all links (left) and only to master links (right).

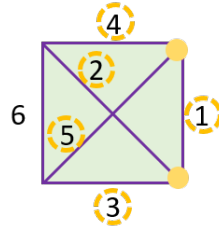


**Fig. 11:** Demonstration of correlated and independent clock observations within a local height system. Here, observation labelled 1 is correlated with all other observations except 6 due to common clock observations. Similarly, the other non-correlated observations are between 3 - 4 and 2 - 5.

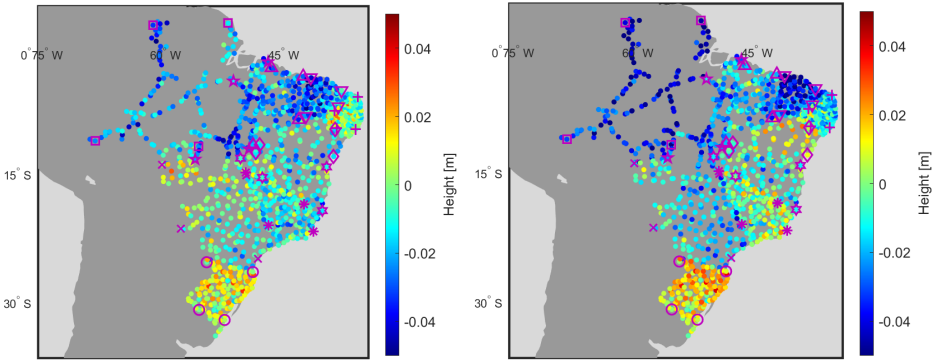


**Fig. 12:** Adjusted errors after reunification with correlation coefficients 0.5 (left) and 0.8 (right). Here,  $CE$  (Clock Error) is supplied as a random normal distribution of constant variance  $0.1 \text{ m}^2/\text{s}^2$  which corresponds to a  $10^{-18}$  clock uncertainty.

We assumed two cases with medium correlation ( $\rho = 0.5$ ) and strong correlation ( $\rho = 0.8$ ) of local clock observations. The rms error after unification increases as we increase the correlation coefficient (Figure 12). The unification accuracy is  $< 3$  cm with ( $\rho = 0.5$ ) and  $< 5$  cm with ( $\rho = 0.8$ ).

### 4.3 European-Brazilian Combined Height System – Relation to the Global Geoid

Now, we consider the European and Brazilian systems as two local systems, LHS1 and LHS2 with local vertical datums NAP and Imbituba, respectively. The unification of LHS1 to LHS2 involves the estimation of the offset,  $OT^{L1}$ . These vertical local

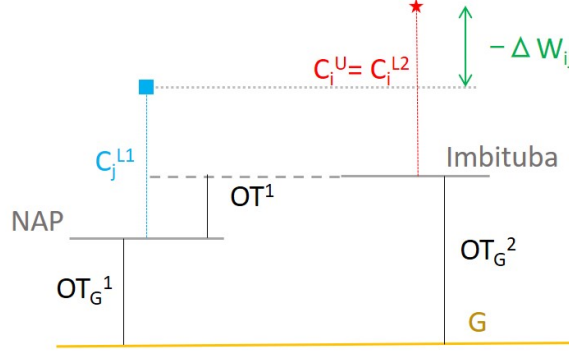


**Fig. 13:** Unification to global geoid using a single clock observation.

datums are not aligned with the global geoid (G). As the offset value of Imbituba to G ( $OT_G^{L2}$ ) is known with a good accuracy of  $\pm 2$  cm [45], unifying LHS1 to LHS2 references all unified heights to G. Also, the offset between NAP to G ( $OT_G^{L1} = OT^{L1} + OT_G^{L2}$ ) can also be estimated. A single clock observation between LHS1 and LHS2 is sufficient as we have only one transformation parameter,  $OT^{L1}$ , to estimate. The equation connecting clock observation to  $OT^{L1}$  is,

$$OT^{L1} = C_j^{L1} - C_i^{L2} - \Delta W_{ij}. \quad (6)$$

Hence, by adding  $OT_G^{L2}$  all heights can be referenced to the geoid with an accuracy of about 3 cm when clocks and links with uncertainties of  $10^{-18}$  are used, which would be better than the present knowledge of about 10 cm [4, 46].

## 5 Conclusion

Our study focuses on a realistic scenario for unifying local height systems through chronometric levelling with high-performance clocks, showing the benefit of clocks in the realisation of the IHRs. To account for various error sources and evaluate the clock performance, we have incorporated complex error parameters into local height



systems. These include datum offsets, local vertical datum alignment discrepancies in latitude and longitude directions, accumulated tilt depending on the distance from the reference tide gauge, and elevation-dependent offsets at levelling points. With the current availability of  $10^{-18}$ -level clocks, which enable a height estimation accuracy of 1 cm, we have investigated various uncertainties associated with clock observations and apply them in our simulation to assess whether the method can achieve a unification accuracy of 1 cm. Realistic daily-averaged clock observations were generated, considering the temporal correlations of intrinsic clock uncertainties, external effects on the clock observations such as tidal effects, propagation delays in terms of link uncertainties, and the presence of outliers. Daily averaging significantly minimizes the tidal effects.

The study demonstrates that an overall 1 cm unification accuracy can be achieved by strategically placing clocks based on tilt and offset characteristics within each local height system. To achieve the best results, clocks should be placed at distant levelling points, reference tide gauges, and elevated locations, ensuring an optimal setup for local height unification. The study demonstrates that 1 cm unification accuracy can still be achieved when using a mixed network of  $10^{-18}$  and  $10^{-17}$  clocks. Strategic clock placement is important for improving error adjustment and achieving high-precision local height system unification. In the proposed clock network configuration with master clocks and local clocks, a unification accuracy of 1 cm can still be achieved with fewer clock links. This reduces observational complexity without significantly compromising accuracy. Further, an outlier model is also implemented to assess the impact of outliers on clock observations, highlighting the need for robust outlier detection and mitigation strategies in real-world applications. The effect of time correlations in clock observations is analyzed, showing that adding correlation degrades the unification accuracy. This underscores the importance of incorporating correlation structures in the covariance matrix using generalized least squares or other advanced statistical methods.

The European and Brazilian height systems can be unified and referenced to the global geoid with an accuracy of 3 cm, significantly improving the current realisations. By incorporating  $10^{-18}$  clocks and similar link uncertainties, the method enables a more accurate global height reference system, enhancing the feasibility of chronometric levelling for future geodetic applications. With the development of portable clocks and proper links, short-term measurement campaigns would be sufficient for the unification process. This approach appears to be practical, reliable and more feasible in the near future.

**Acknowledgements.** This study has been funded by the Deutsche Forschungsgemeinschaft (DFG, German Research Foundation) under Germany’s Excellence Strategy EXC 2123 Quantum Frontiers – Project-ID 90837967, SFB 1464 TerraQ – Project-ID 434617780, and FOR 5456: Clock Metrology: A Novel Approach to TIME in Geodesy – Project-ID 490990195.

**Data Availability Statement.** The datasets generated and analyzed during the current study are available from the corresponding author upon reasonable request.

**Author Contributions.** J.M. stimulated the study and provided the basic ideas. A.V. conceived the study, developed the methodology, and performed all simulations. A.V. and J.M. analyzed the results. A.V. wrote the first draft of the manuscript. C.L. provided input on the error behaviour of optical clocks. D.P. checked and optimised the relativity parts. All authors contributed to the interpretation of the data, reviewed the manuscript, and approved the final version.

## Declarations

We thank Dr. Eng. Gabriel Guimarães, chair of the SIRGAS Working Group III (Vertical Datum), for providing the Brazilian levelling data.

## References

- [1] Sánchez, L., Ågren, J., Huang, J., Wang, Y.M., Mäkinen, J., Pail, R., Barzaghi, R., Vergos, G.S., Ahlgren, K., Liu, Q.: Strategy for the realisation of the international height reference system (ihrs). *Journal of Geodesy* **95**(3), 1–33 (2021)
- [2] Delva, P., Denker, H., Lion, G.: In: Puetzfeld, D., Lämmerzahl, C. (eds.) *Chronometric Geodesy: Methods and Applications*, pp. 25–85. Springer, Cham (2019). [https://doi.org/10.1007/978-3-030-11500-5\\_2](https://doi.org/10.1007/978-3-030-11500-5_2) . [https://doi.org/10.1007/978-3-030-11500-5\\_2](https://doi.org/10.1007/978-3-030-11500-5_2)
- [3] Müller, J., Soffel, M., Klioner, S.A.: Geodesy and relativity. *Journal of Geodesy* **82**, 133–145 (2008)
- [4] Ihde, J., Sánchez, L., Barzaghi, R., Drewes, H., Foerste, C., Gruber, T., Liebsch, G., Marti, U., Pail, R., Sideris, M.: Definition and proposed realization of the international height reference system (ihrs). *Surveys in geophysics* **38**, 549–570 (2017)
- [5] Wu, H., Müller, J., Lämmerzahl, C.: Clock networks for height system unification: a simulation study. *Geophysical Journal International* **216**(3), 1594–1607 (2018) <https://doi.org/10.1093/gji/ggy508> <https://academic.oup.com/gji/article-pdf/216/3/1594/27226427/ggy508.pdf>
- [6] Wu, H., Müller, J.: Towards an international height reference frame using clock networks. In: Freymüller, J.T., Sánchez, L. (eds.) *Beyond 100: The Next Century in Geodesy*, pp. 3–10. Springer, Cham (2022)
- [7] Vincent, A., Müller, J.: Detection of time variable gravity signals using terrestrial clock networks. *Advances in Space Research* (2023) <https://doi.org/10.1016/j.asr.2023.07.058>
- [8] Vincent, A., Müller, J.: Vision of a Clock-Based Network for Absolute Sea Level Monitoring, pp. 1–8. Springer, Berlin, Heidelberg (2024). [https://doi.org/10.1007/978-3-031-41111-1\\_1](https://doi.org/10.1007/978-3-031-41111-1_1)

- [9] Sánchez, L., Wziontek, H., Wang, Y.M., Vergos, G., Timmen, L.: Towards an integrated global geodetic reference frame: preface to the special issue on reference systems in physical geodesy. *Journal of Geodesy* **97**(6), 59 (2023)
- [10] Drewes, H., Kuglitsch, F.G., Adám, J., Rózsa, S.: The geodesist's handbook 2016. *Journal of geodesy* **90**(10), 907–1205 (2016)
- [11] Jekeli, C.: Heights, the geopotential, and vertical datums (2000)
- [12] Bjerhammar, A.: On a relativistic geodesy. *Bulletin géodésique* **59**(3), 207–220 (1985) <https://doi.org/10.1007/BF02520327>
- [13] Müller, J., Dirkx, D., Kopeikin, S.M., Lion, G., Panet, I., Petit, G., Visser, P.: High performance clocks and gravity field determination. *Space Science Reviews* **214**(1), 1–31 (2018) <https://doi.org/10.1007/s11214-017-0431-z>
- [14] Denker, H., Timmen, L., Voigt, C., Weyers, S., Peik, E., Margolis, H.S., Delva, P., Wolf, P., Petit, G.: Geodetic methods to determine the relativistic redshift at the level of  $10^{-18}$  in the context of international timescales: a review and practical results. *Journal of Geodesy* **92**(5), 487–516 (2018) <https://doi.org/10.1007/s00190-017-1075-1>
- [15] Pavlis, N.K., Weiss, M.A.: The relativistic redshift with  $3 \times 10^{-17}$  uncertainty at nist, boulder, colorado, usa. *Metrologia* **40**(2), 66 (2003)
- [16] Pavlis, N.K., Weiss, M.A.: A re-evaluation of the relativistic redshift on frequency standards at nist, boulder, colorado, usa. *Metrologia* **54**(4), 535 (2017)
- [17] Philipp, D., Perlick, V., Puetzfeld, D., Hackmann, E., Lämmerzahl, C.: Definition of the relativistic geoid in terms of isochronometric surfaces. *Phys. Rev. D* **95**, 104037 (2017) <https://doi.org/10.1103/PhysRevD.95.104037>
- [18] Philipp, D., Hackmann, E., Lämmerzahl, C., Müller, J.: Relativistic geoid: Gravity potential and relativistic effects. *Phys. Rev. D* **101**, 064032 (2020) <https://doi.org/10.1103/PhysRevD.101.064032>
- [19] Sanner, C., Huntemann, N., Lange, R., Tamm, C., Peik, E., Safronova, M.S., Porsev, S.G.: Optical clock comparison for lorentz symmetry testing. *Nature* **567**(7747), 204–208 (2019)
- [20] Collaboration, B.A.C.O.N.B., *et al.*: Frequency ratio measurements at 18-digit accuracy using an optical clock network. *Nature* **591**(7851), 564–569 (2021)
- [21] Arnold, K.J., Bustabad, S., Qichen, Q., Zhang, Z., Zhao, Q., Barrett, M.D.: Validating a lutetium frequency reference. *J. Phys.: Conf. Ser.* **2889**, 012040 (2024) <https://doi.org/10.1088/1742-6596/2889/1/012040>

- [22] McGrew, W., Zhang, X., Fasano, R., Schäffer, S., Beloy, K., Nicolodi, D., Brown, R., Hinkley, N., Milani, G., Schioppo, M., *et al.*: Atomic clock performance enabling geodesy below the centimetre level. *Nature* **564**(7734), 87–90 (2018) <https://doi.org/10.1038/s41586-018-0738-2>
- [23] Bothwell, T., Kennedy, C.J., Aeppli, A., Kedar, D., Robinson, J.M., Oelker, E., Staron, A., Ye, J.: Resolving the gravitational redshift across a millimetre-scale atomic sample. *Nature* **602**(7897), 420–424 (2022)
- [24] Ihde, J., Adam, J., Gurtner, W., Harsson, B., Sacher, M., Schlüter, W., Wöppelmann, G.: The height solution of the european vertical reference network (euvn). *Veröff. Bayer. Komm. für die Internat. Erdmessung, Astronom. Geod. Arb* **61**, 132–145 (2000)
- [25] Williams, P.A., Swann, W.C., Newbury, N.R.: High-stability transfer of an optical frequency over long fiber-optic links. *JOSA B* **25**(8), 1284–1293 (2008)
- [26] Lisdat, C., Grosche, G., Quintin, N., Shi, C., Raupach, S., Grebing, C., Nicolodi, D., Stefani, F., Al-Masoudi, A., Dörscher, S., *et al.*: A clock network for geodesy and fundamental science. *Nature communications* **7**(1), 12443 (2016)
- [27] Koke, S., Kuhl, A., Waterholter, T., Raupach, S.M.F., Lopez, O., Cantin, E., Quintin, N., Amy-Klein, A., Pottier, P.-E., Grosche, G.: Combining fiber Brillouin amplification with a repeater laser station for fiber-based optical frequency dissemination over 1400 km. *New J. Phys.* **21**(12), 123017 (2019) <https://doi.org/10.1088/1367-2630/ab5d95>
- [28] Riedel, F., Al-Masoudi, A., Benkler, E., Dörscher, S., Gerginov, V., Grebing, C., Häfner, S., Huntemann, N., Lipphardt, B., Lisdat, C., Peik, E., Piester, D., Sanner, C., Tamm, C., Weyers, S., Denker, H., Timmen, L., Voigt, C., Calonico, D., Cerretto, G., Costanzo, G.A., Levi, F., Sesia, I., Achkar, J., Guéna, J., Abgrall, M., Rovera, G.D., Chupin, B., Shi, C., Bilicki, S., Bookjans, E., Lodewyck, J., Le Targat, R., Delva, P., Bize, S., Baynes, F.N., Baynham, C., Bowden, W., Gill, P., Godun, R.M., Hill, I.R., Hobson, R., Jones, J.M., King, S.A., Nisbet-Jones, P., Rolland, A., Shemar, S.L., Whibberley, P.B., Margolis, H.S.: Direct comparisons of European primary and secondary frequency standards via satellite techniques. *Metrologia* **57**(4), 045005 (2020) <https://doi.org/10.1088/1681-7575/ab6745>
- [29] Fujieda, M., Yang, S.-H., Gotoh, T., Hwang, S.-W., Hachisu, H., Kim, H., Lee, Y.K., Tabuchi, R., Ido, T., Lee, W.-K., Heo, M.-S., Park, C.Y., Yu, D.-H., Petit, G.: Advanced satellite-based frequency transfer at the  $10^{-16}$  level. *IEEE Trans. Ultrason. Ferroelectr. Freq. Control* **6**, 973–978 (2018) <https://doi.org/10.1109/TUFFC.2018.2821159>
- [30] Jian, B., Beattie, S., Weyers, S., Rahm, J., Donahue, B., Gertsvolf, M.: GPS PPP-AR frequency transfer and its application for comparing atomic fountain primary frequency standards between NRC and PTB. *Metrologia* **60**(6), 065002

- (2023) <https://doi.org/10.1088/1681-7575/acfa04>
- [31] Caldwell, E.D., Deschenes, J.-D., Ellis, J., Swann, W.C., Stuhl, B.K., Bergeron, H., Newbury, N.R., Sinclair, L.C.: Quantum-limited optical time transfer for future geosynchronous links. *Nature* **618**(7966), 721–726 (2023) <https://doi.org/10.1038/s41586-023-06032-5>
  - [32] Rovera, G.D., Abgrall, M., Courde, C., Exertier, P., Fridelance, P., Guillemot, P., Laas-Bourez, M., Martin, N., Samain, E., Sherwood, R., Torre, J.-M., Urich, P.: A direct comparison between two independently calibrated time transfer techniques: T2L2 and GPS common-views. *J. Phys.: Conf. Ser.* **723**(1), 012037 (2016) <https://doi.org/10.1088/1742-6596/723/1/012037>
  - [33] Cacciapuoti, L., Salomon, C.: Atomic clock ensemble in space. *Journal of Physics: Conference Series* **327**, 012049 (2011)
  - [34] Shen, Z., Shen, W., Xu, X., Zhang, S., Zhang, T., He, L., Cai, Z., Xiong, S., Wang, L.: A method for measuring gravitational potential of satellite’s orbit using frequency signal transfer technique between satellites. *Remote Sensing* **15**(14), 3514 (2023)
  - [35] Jentzsch, G.: Earth tides and ocean tidal loading. *Tidal phenomena*, 145–171 (2005)
  - [36] McCarthy, D.D., Luzum, B.J.: An analysis of tidal variations in the length of day. *Geophysical Journal International* **114**(2), 341–346 (1993)
  - [37] Lindzen, R.S., Chapman, S.: Atmospheric tides. *Space science reviews* **10**, 3–188 (1969)
  - [38] Voigt, C., Denker, H., Timmen, L.: Time-variable gravity potential components for optical clock comparisons and the definition of international time scales. *Metrologia* **53**(6), 1365 (2016) <https://doi.org/10.1088/0026-1394/53/6/1365>
  - [39] Wenzel, H.-G.: Eterna - Programs for tidal analysis and prediction (2022). <https://doi.org/10.35097/746>
  - [40] DGFI-Report No.89: Savcenko R, B.W.: Eot11a - empirical ocean tide model from multi-mission satellite altimetry. Technical report, DGFI-TUM (2012)
  - [41] Agnew, D.C.: Spotl: Some programs for ocean-tide loading (2012)
  - [42] Gruber, T., Rummel, R., Ihde, J., Liebsch, G., Rülke, A., Schäfer, U., Sideris, M., Rangelova, L., Woodworth, P.: Height system unification with goce summary and final report. Technical report, Technical Report GO-HSU-PL-0021 (2014)
  - [43] Fotopoulos, G., Kotsakis, C., Sideris, M.G.: How accurately can we determine orthometric height differences from gps and geoid data? *Journal of surveying*

engineering **129**(1), 1–10 (2003)

- [44] Huber, P.J.: In: Lovric, M. (ed.) Robust Statistics, pp. 1248–1251. Springer, Berlin, Heidelberg (2011). [https://doi.org/10.1007/978-3-642-04898-2\\_594](https://doi.org/10.1007/978-3-642-04898-2_594) .  
[https://doi.org/10.1007/978-3-642-04898-2\\_594](https://doi.org/10.1007/978-3-642-04898-2_594)
- [45] Sánchez, L., Sideris, M.G.: Vertical datum unification for the International Height Reference System (IHRs). Geophysical Journal International **209**(2), 570–586 (2017) <https://doi.org/10.1093/gji/ggx025>  
<https://academic.oup.com/gji/article-pdf/209/2/570/10851543/ggx025.pdf>
- [46] Woodworth, P., Hughes, C., Bingham, R., Gruber, T.: Towards worldwide height system unification using ocean information. Journal of Geodetic Science **2**(4), 302–318 (2012)